

Modelling the dynamics of online food delivery services on the spread of food-borne diseases

Emmanuel Addai^a, Delfim F. M. Torres^{b,c}, Zalia Abdul-Hamid^d, Mary Nwaife Mezue^a,
Joshua Kiddy K. Asamoah^{e,f,*}

^aCollege of Computer and Information Science, University of Arkansas at Little Rock, 72204 Little Rock, Arkansas, USA

^bCenter for Research and Development in Mathematics and Applications (CIDMA),

Department of Mathematics, University of Aveiro, 3810-193 Aveiro, Portugal

^cResearch Center in Exact Sciences (CICE), Faculty of Sciences and Technology (FCT),

University of Cape Verde (Uni-CV), 7943-010 Praia, Cabo Verde

^dDepartment of Logistics and Sustainable Transport, University of Maryland, 20740 College Park, Maryland, USA

^eDepartment of Mathematics, Saveetha School of Engineering SIMATS, Chennai, India

^fDepartment of Mathematics, Kwame Nkrumah University of Science and Technology, Kumasi, Ghana

Abstract

We propose and analyze a deterministic mathematical model for the transmission of food-borne diseases in a population consisting of humans and flies. We employ the Caputo operator to examine the impact of governmental actions and online food delivery services on the transmission of food-borne diseases. The proposed model investigates important aspects such as positivity, boundedness, disease-free equilibrium, basic reproduction number and sensitivity analysis. The existence and uniqueness of a solution for the initial value problem is established using Banach and Schauder type fixed point theorems. Functional techniques are employed to demonstrate the stability of the proposed model under the Hyers-Ulam condition. For an approximate solution, the iterative fractional order Predictor-Corrector scheme is utilized. The simulation of this scheme is conducted using Matlab as the numeric computing environment, with various fractional order values ranging from 0.75 to 1. Over time, all compartments demonstrate convergence and stability. The numerical simulations highlight the necessity for the government to implement the most effective food safety control interventions. These measures could involve food safety awareness and training campaigns targeting restaurant managers, staff members involved in online food delivery, as well as food delivery personnel.

Keywords: Mathematical modelling, Food-borne diseases transmission, Online food delivery, Caputo fractional derivatives, Numerical simulations.

2020 MSC: 26A33; 34D20; 37M05; 92B05.

*Corresponding Author

Email addresses: eaddai1@ualr.edu; papayawewit@gmail.com (Emmanuel Addai), delfim@ua.pt; delfim@unicv.cv (Delfim F. M. Torres), zaliaabdulhamid96@gmail.com (Zalia Abdul-Hamid), Mezuemary@gmail.com (Mary Nwaife Mezue), jkkasamoah@knust.edu.gh (Joshua Kiddy K. Asamoah)

1. Introduction

Urbanisation, non-communicable diseases, unhealthy diets, and climate change are all acknowledged as major threats to world health [25]. In order to promote healthy lives and well-being and create inclusive, secure, and sustainable cities by 2030, the United Nations has asked all of its member states to take action on 17 Sustainable Development Goals (SDGs) spanning economic, social, and environmental dimensions [46]. Online food delivery services (OFDS) have the potential to impede our progress towards the SDGs by affecting our eating, working, and environmental practises. OFDS provide delivery of a wide range of takeaway foods and beverages from kitchens to doorsteps and are described as platform-to-consumer delivery operations of ready-to-consume meals [42]. These include of dishes such as pizza, burgers, sandwiches, wraps, spaghetti, and pides. Currently, the Online Food Delivery Service (OFDS) industry is largely controlled by major international corporations with a global footprint. The practice of ordering ready-to-eat meals online introduces new and additional risks to food safety, compounded by the growing reach and prevalence of OFDS. These risks stem from the involvement of delivery personnel in the supply chain, acting as intermediaries between food producers and the end consumers. For example, when the consumer is not present at the point of sale, such as a restaurant, it opens opportunities for fraudulent activities like swapping or mislabeling products, aiming to profit by substituting high-quality items with substandard alternatives [43].

Over the past few decades, concerted efforts by food suppliers, industries, and regulatory bodies have been instrumental in elevating food production standards to meet rigorous health requirements. This has been pivotal in curbing the public health risks and financial repercussions associated with foodborne illnesses. Numerous initiatives and programs have been put in place globally by both governmental entities and the private sector to realize this objective. Despite these advances, foodborne diseases triggered by various agents like bacteria (*E. coli*, *Salmonella*, *Campylobacter*, *Listeria*, *Clostridium perfringens*), viruses (Norovirus), natural toxins, and chemical contaminants-continue to pose significant health threats internationally. This is due to the continuous emergence of new hazards while existing ones are being managed.

Recently, the study of infectious disease dynamics has expanded significantly, developing into a complex, interdisciplinary domain that includes epidemiology, public health, and beyond [47], [33]. This area brings together a wide range of academic disciplines such as sociology, machine learning, artificial neural networks, mathematics, and biology to understand and predict the spread of diseases and various social behavioral issues [39]–[48]. Mathematical models are pivotal in epidemiology, which focuses on how diseases spread. These models apply mathematical principles to depict the dissemination of diseases and their effects on populations. They are essential tools for research, enabling scientists to formulate and test hy-

potheses, assess quantitative theories, address specific questions, evaluate the effects of parameter changes, and calculate vital parameters using mathematical modeling and computer simulations [24, 31, 37]. For many years, mathematical models have helped researchers and public health practitioners to predict the potential impact of disease outbreaks, identify the key drivers of outbreaks, and evaluate the effectiveness of different control strategies. Although much research based on mathematical modelling has been done contributing to fight food-borne diseases, the most worrying aspect about it is that we are yet far-reaching from the accurate and high degree of prediction [32, 22, 26]. As a result, it is critical to improve our understanding of the dynamics of food-borne transmission by incorporating novel methods into the current models. Insights into the spread and management of numerous viral infectious diseases around the world have long been obtained using mathematical modelling [7, 9, 10]. The study conducted by [29] employed a mathematical model to investigate how the behaviours of honeybees can decrease the likelihood of outbreaks of deformed wing virus in colonies afflicted with *Varroa destructor*. The paper by [1] investigated the optimal and cost-effective regulation of drug addiction among students using mathematical modelling. The paper by [6] introduced a mathematical model that describes the dynamics of Chikungunya virus within a host, taking into account the adaptive immune response. The SDIQR mathematical model of COVID-19 is utilised by LADT to examine numerical data regarding infected migrants in Odisha. The COVID-19 model in the work of [38] utilises analytical power series and LADT to estimate the solution profiles of dynamical variables. The research undertaken by [34] centres on the creation and examination of a deterministic mathematical model for the monkeypox virus. The criteria for achieving both local and global stability of disease-free and endemic equilibria are established. The evidence suggests that the model undergoes a backward bifurcation, where the disease-free equilibrium, which is stable in the local context, coexists with an endemic equilibrium. The research undertaken by [8] presented a mathematical model that combines the memory effect to mimic the transmission of HIV in a heterosexual population. The population is divided into two age cohorts: the youth cohort, comprising those aged 15–24, and the adult cohort, comprising individuals aged 25 and above. The purpose of classifying the population by age is to identify the most vulnerable group to the virus based on their sexual behaviour and produce accurate predictions on HIV transmission. A study conducted by [3] devised an optimal control system that integrated three strategies (public awareness campaign, post-exposure vaccination, and isolation) to determine the most efficient combination for substantially lowering or eradicating disease transmission. We have proven the existence of optimum control and identified the necessary conditions for optimality through the application of Pontryagin’s notion. Mathematical models based on traditional integer-order dynamics have been extensively applied in epidemiology due to their success in describing disease spread, see [16] and the references therein. Nevertheless, it is becoming increasingly recognized that these mod-

els may not sufficiently account for complex phenomena such as hereditary characteristics, long-distance interactions, and memory effects, which are prevalent across various scientific and engineering disciplines, see [15, 17, 18, 20, 21] and the references therein.

In contrast, models employing fractional-order differential operators are gaining favor for their enhanced ability to depict the intricate behaviors of dynamic systems. Fractional models are particularly adept at incorporating memory and hereditary attributes, offering a more nuanced understanding of disease dynamics. This attribute makes them exceptionally relevant for a more accurate simulation of biological processes and other fields where these complex dynamics are significant [19].

Fractional order differential problems are now one of the most effective and practical methods for modelling nonlinear processes that appear in innumerable applications in real-world settings. Recently, the discipline of mathematical biology has begun to apply several types of fractional order derivatives. These operators have recently appear in numerous works, for instance, in mathematical models for HIV/AIDS [14], Ebola-malaria co-infection models [49], smoke age-specific models [2], monkeypox transmission dynamics [35], Middle East Lungs Coronavirus dynamism transmission models [5], COVID-19 models [28], and Hepatitis E disease models [27]. For more applications of fractional differential equations see, e.g., [30, 4] and references therein. Furthermore, in the context of food-borne diseases transmission dynamics, the authors in [40] used fractional q -Homotopy analysis transformations to study food-borne disease model and suggested control policies that help the general public comprehension of the importance of control parameters in the extinction of the diseases. In fact, this study has accurately predicted the food-borne diseases transmission dynamics and the impact of government intervention and online food delivery services on the outbreak, allowing for a more accurate representation of the underlying disease dynamics. However, none of them, to the best of our knowledge, have studied the effects of government intervention and online food delivery services on the dynamics of food-borne diseases transmission using fractional-order derivatives.

The primary goal of this study is to develop and analyze a fractional-order epidemic model using the Caputo definition, to assess the impact of governmental measures and online food delivery services on controlling the spread of food-borne diseases. The Caputo fractional-order derivative is chosen for its ability to incorporate conventional initial conditions into the model's solution, making parameter estimation more precise due to its inherent memory capability. The structure of the paper is methodically laid out to facilitate understanding and exploration of the model. Definitions and necessary preliminary information form the basis of Sect.2, setting the stage for the subsequent analysis. Sect. 3 is dedicated to the method of the study, the detailed construction of the model pertaining to the transmission of food-borne diseases. Further, explores the equilibrium states and the basic reproduction number – key

concepts in understanding the potential spread of an infection. The mathematical rigor continues, which verifies the unique solutions to the proposed model. We discuss the stability of these solutions, an essential aspect of predicting the long-term behavior of the disease transmission. The paper then moves into more applied aspects in Sect. 4, where the numerical techniques used in the study are outlined. In Sect. 5 we present the results of the study by simulations that demonstrate the practical implications of the model. In Sect. 6 we present the discussion of the study. Finally, the paper wraps up with conclusions in Sect. 7, which summarize the findings and their relevance to public health policy and disease control measures.

2. Preliminaries

We recall the necessary definitions of fractional derivative and fractional integral and a lemma that is important in our proofs.

Definition 2.1 (See [36]). *Let $\mathcal{M} : \mathbb{R}^+ \rightarrow \mathbb{R}$ and $\alpha \in (n-1, n)$, $n \in \mathbb{N}$. Then, one can define the Caputo derivative with order α for the function \mathcal{M} by*

$${}_0^C D_t^\alpha \mathcal{M}(t) = \frac{1}{\Gamma(n-\alpha)} \int_0^t (t-s)^{n-\alpha-1} \mathcal{M}^{(n)}(s) ds. \quad (1)$$

Definition 2.2 (See [36]). *The related fractional integral is given by*

$${}_0^C I_t^\alpha \mathcal{M}(t) = \frac{1}{\Gamma(\alpha)} \int_0^t (t-s)^{\alpha-1} \mathcal{M}(s) ds. \quad (2)$$

Lemma 2.1 (See [44, 41]). *Consider a function $\mathcal{M} \in C[0, \mathcal{T}]$. The solution of the fractional differential equation*

$$\begin{cases} {}_0^C D_t^\alpha \mathcal{M}(t) = \Phi(t), & t \in [0, \eta], \\ \mathcal{M}(0) = \mathcal{M}_0, \end{cases} \quad (3)$$

is given by

$$\mathcal{M}(t) = \mathcal{M}(0) + \frac{1}{\Gamma(\alpha)} \int_0^t \Phi(s, \mathcal{M}(s)) (t-s)^{\alpha-1} ds. \quad (4)$$

3. Method

3.1. Model Formulation

In this section, we present the formulation of our model. For this, we consider both human and flies populations in a closed homogeneous environment. For a human population at a time t , we consider five compartments: Susceptible humans $S(t)$; Asymptomatic infected humans $A(t)$; Symptomatic infected humans $I(t)$; Online food delivery personals $D(t)$. For the human population, we define the quantity N_h (total human population) by

$$N_h(t) = S(t) + A(t) + I(t) + D(t). \quad (5)$$

Now we describe the three compartments of flies: pupae of flies $P_f(t)$, adult flies population $G_f(t)$, and parasitic wasps population $W_p(t)$. The flies population, as a whole, is given by

$$N_f(t) = P_f(t) + G_f(t) + W_p(t). \quad (6)$$

We assume that individuals have no permanent recovery. Asymptomatic individuals who develop temporal resistance to the disease become susceptible again at the rate ξ . The value $\xi = 0$ indicates no temporal resistance to the disease, while $\xi = 1$ indicates 100% resistance to the disease, which means that no infection occurs ($I(t) \equiv 0$). We model local government interventions by a control $u(t)$, which depends on time t and take values between zero and one. We assume that there is no local government intervention when $u(t) = 0$, while $u(t) = 1$ represents perfect or maximum intervention. Considering the interrelationship, we formulate the following deterministic system of nonlinear differential equations:

$$\left\{ \begin{array}{l} \frac{dS(t)}{dt} = \Pi + \xi A - (1 - u)\lambda S - \mu_h S, \\ \frac{dA(t)}{dt} = (1 - u)\lambda S - (\mu_h + \eta + \xi)A, \\ \frac{dI(t)}{dt} = \eta A - (\mu_h + \delta)I, \\ \frac{dD(t)}{dt} = \psi(A + I) - ((1 - u) + \theta + \gamma)D, \\ \frac{dP_f(t)}{dt} = \sigma G_f - (\rho + \mu_f)P_f - \tau P_f W_p, \\ \frac{dG_f(t)}{dt} = \rho P_f - \mu_f G_f, \\ \frac{dW_p(t)}{dt} = \kappa \tau P_f W_p - \mu_f W_p, \end{array} \right. \quad (7)$$

subject to given initial conditions

$$S(0) = S_0 \geq 0, \quad A(0) = A_0 \geq 0, \quad I(0) = I_0 \geq 0, \quad D(0) = D_0 \geq 0, \quad (8)$$

$$P_f(0) = P_{f_0} \geq 0, \quad G_f(0) = G_{f_0} \geq 0, \quad W_p(0) = W_{p_0} \geq 0, \quad (9)$$

where $\lambda = \frac{\beta(rA+I)D}{N_h} + \vartheta G_f$ and $t > 0$. The flow diagram of the model is presented in Fig. 1, while the description of the parameters is presented in Table 1. Table 1 also contains values that is for the numerical simulations.

According to the explanations of the time-dependent kernel defined by the power law correlation function, presented in [45], one can take into consideration the Caputo fractional order derivative on our proposed model:

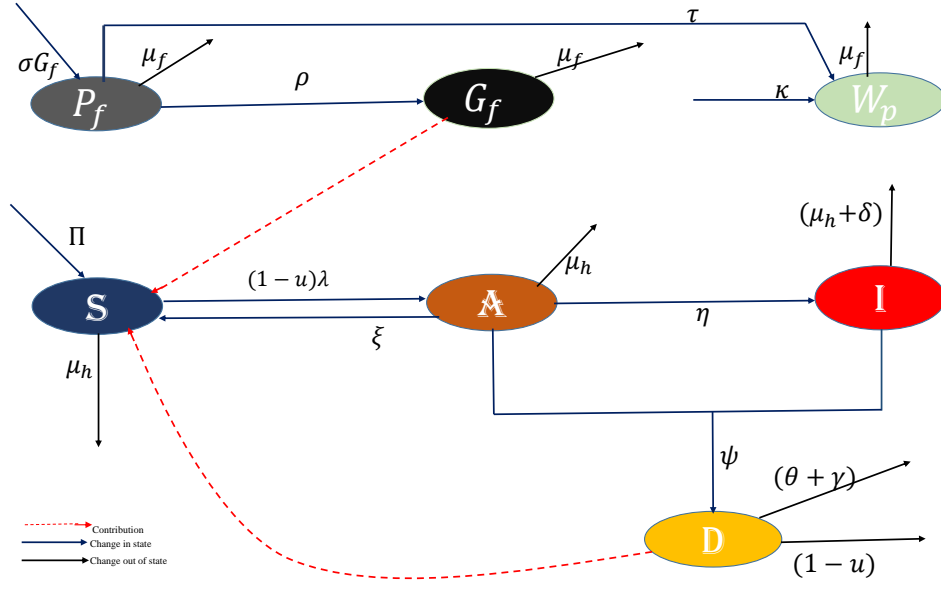


Fig. 1: Transfer diagram for the dynamic transmission of food-borne diseases given by model (7).

Table 1: Interpretation of the parameters of model (7).

Parameter	value	Interpretation	value
Π	1000	recruitment rate of human	Assumed
ξ	$0.0021 \text{ (day}^{-1}\text{)}$	temporal resistance rate	Assumed
β	$0.0014 \text{ (day}^{-1}\text{)}$	effective contact rate	Assumed
θ	$0.50 \text{ (day}^{-1}\text{)}$	the rate of environmental hygiene	[40]
γ	$0.001 \text{ (day}^{-1}\text{)}$	the rate of $A(t)$ fail to deliver food ordered	[40]
r	$0.0016667 \text{ (day}^{-1}\text{)}$	progression rate from $A(t)$ to $I(t)$	Assumed
μ_h, μ_f	$1/87.7, 0.000233 \text{ (day}^{-1}\text{)}$	natural death rate for human and flies	[40]
η	$0.000375 \text{ (day}^{-1}\text{)}$	the rate at which the asymptomatic become infected	Assumed
δ	$0.01 \text{ (day}^{-1}\text{)}$	disease induced death rate	Assumed
ψ	$0.47 \text{ (day}^{-1}\text{)}$	the rate of disease inflow by both $A(t)$ and $I(t)$	Assumed
σ	$0.019 \text{ (day}^{-1}\text{)}$	the rate of adult fly lay egg in the environment	[40]
ρ	$0.003 \text{ (day}^{-1}\text{)}$	the rate at which $P_f(t)$ move to $G_f(t)$	[40]
τ	$0.0021 \text{ (day}^{-1}\text{)}$	reduction coefficient of $P_f(t)$ and $W_p(t)$ due to the interaction	Assumed
κ	$0.01 \text{ (day}^{-1}\text{)}$	proportionality constant	[40]

$$\begin{cases} {}^C_0 D_t^\alpha S(t) = \Pi + \xi A - (1-u)\lambda S - \mu_h S, \\ {}^C_0 D_t^\alpha A(t) = (1-u)\lambda S - (\mu_h + \eta + \xi)A, \\ {}^C_0 D_t^\alpha I(t) = \eta A - (\mu_h + \delta)I, \\ {}^C_0 D_t^\alpha D(t) = \psi(A + I) - ((1-u) + \theta + \gamma)D, \\ {}^C_0 D_t^\alpha P_f(t) = \sigma G_f - (\rho + \mu_f)P_f - \tau P_f W_p, \\ {}^C_0 D_t^\alpha G_f(t) = \rho P_f - \mu_f G_f, \\ {}^C_0 D_t^\alpha W_p(t) = \kappa \tau P_f W_p - \mu_f W_p, \end{cases} \quad (10)$$

where $t \in [0, \mathcal{T}]$, $\mathcal{T} \in \mathbb{R}$, and ${}^C_0 D_t^\alpha$ denotes the Caputo fractional derivative of order $0 < \alpha \leq 1$. Note that when $\alpha = 1$ the fractional-order model (10) reduces to (7).

3.2. Fundamental Qualitative Properties of the Model

Now, we prove positivity and boundedness of the solution to the proposed model and we obtain the corresponding basic reproduction number.

3.3. Positivity and boundedness

Here, we demonstrate the epidemiological significance of the model under consideration. We prove that the system classes for model (7) are non-negative for all t , which means that our suggested model has, for all $t > 0$, non-negative solutions for non-negative initial values.

Lemma 3.1. *Let*

$$\mathcal{M}(t) = \{(S(t), A(t), I(t), D(t), P_f(t), G_f(t), W_p(t)) \in \mathbb{R}^7\}, \quad t \geq 0, \quad (11)$$

and $\mathcal{T} \in \mathbb{R}$. If the initial data is positive, that is, $\mathcal{M}(0) > 0$, then the solution classes of model (7) are non-negative in $[0, \mathcal{T}]$. Also,

$$\lim_{t \rightarrow \infty} N_h(t) \leq \frac{\Pi}{\mu_h}, \quad (12)$$

and

$$\lim_{t \rightarrow \infty} N_f(t) \leq \frac{\sigma}{\mu_f}, \quad (13)$$

with N_h and N_f given by (5) and (6), respectively.

Proof. Take $t_1 = \sup\{t > 0 : \mathcal{M}(t) > 0 \forall t \in [0, \mathcal{T}]\}$ and let us consider the first dynamical equation of model (7):

$$\frac{dS(t)}{dt} = \Pi + \xi A - (1-u)\lambda S - \mu_h S. \quad (14)$$

For simplicity, let

$$\mathcal{Y} = [(1-u)\lambda - \mu_h] \quad (15)$$

. Thus,

$$\frac{dS(t)}{dt} + \mathcal{Y}S(t) = \Pi + \xi A. \quad (16)$$

This leads to

$$\frac{d}{dt} \left(S(t) \exp \left(\int_0^{t_1} \mathcal{Y}(s) ds \right) \right) = (\Pi + \xi A) \exp \left(\int_0^{t_1} \mathcal{Y}(s) ds \right), \quad (17)$$

and

$$S(t) = \exp \left(- \int_0^{t_1} \mathcal{Y}(s) ds \right) \left[\int_0^{t_1} (\Pi + \xi A) \exp \left(\int_0^{t_1} \mathcal{Y}(s) ds \right) \right]. \quad (18)$$

Hence, we proved that $S(0) > 0$ for all $t > 0$. Similarly, from the other classes of model (7), we can get $\mathcal{M}(0) > 0$ for all $t > 0$. Note that after the summation of the state variables in model (7), we have

$$\begin{aligned} \frac{dN_h(t)}{dt} &= \Pi - \mu_h N_h(t), \\ \frac{dN_f(t)}{dt} &= \sigma - \mu_f N_f(t). \end{aligned} \quad (19)$$

Hence, $\lim_{t \rightarrow \infty} N_h(t) \leq \frac{\Pi}{\mu_h}$ and $\lim_{t \rightarrow \infty} N_f(t) \leq \frac{\sigma}{\mu_f}$, which completes the proof. \square

For feasibility of model (7), we let $\mathcal{X} = \Omega_h + \Omega_F \subset \mathbb{R}_+^1 \times \mathbb{R}_+^2$, where

$$\mathcal{X} = \left\{ (S, A, I, D, P_f, G_f, W_p) \in \mathbb{R}_+^7 : N_h(t) \leq \frac{\Pi}{\mu_h}, N_f(t) \leq \frac{\sigma}{\mu_f} \right\}. \quad (20)$$

In solving the inequalities above we have

$$\begin{aligned} N_h(t) &\leq N_h(0)e^{-\mu_h t} + \frac{\Pi}{\mu_h} (1 - e^{-\mu_h t}), \\ N_f(t) &\leq N_f(0)e^{-\mu_f t} + \frac{\sigma}{\mu_f} (1 - e^{-\mu_f t}). \end{aligned} \quad (21)$$

Therefore,

$$\begin{aligned} \limsup_{t \rightarrow \infty} N_h(t) &\leq \frac{\Pi}{\mu_h}, \\ \limsup_{t \rightarrow \infty} N_f(t) &\leq \frac{\sigma}{\mu_f}. \end{aligned} \quad (22)$$

Hence, our proposed model (7) is considered to be mathematically well posed.

For positivity of model (10), we add all the state variables in model (10) to get

$$\begin{aligned} {}^C_0 D_t^\alpha N_h(t) &= \Pi - \mu_h N_h(t), \\ {}^C_0 D_t^\alpha N_f(t) &= \sigma - \mu_f N_f(t), \end{aligned} \quad (23)$$

from which we conclude that (22) also holds for (10), showing that model (10) remains in the feasible region \mathcal{X} .

3.4. Food-borne diseases reproduction number and the disease-free equilibrium

For the parameters of our model (7), let $k_1 = \mu_h + \eta + \xi$, $k_2 = \mu_h + \delta$, $k_3 = 1 - u + \theta + \gamma$, and $k_4 = \rho + \mu_f$. Equating the right-hand side of the proposed model (7) to zero, that is,

$$\begin{cases} \Pi + \xi A - (1 - u)\lambda S - \mu_h S = 0, \\ (1 - u)\lambda S - (\mu_h + \eta + \xi)A = 0, \\ \eta A - (\mu_h + \delta)I = 0, \\ \psi(A + I) - ((1 - u) + \theta + \gamma)D = 0, \\ \sigma G_f - (\rho + \mu_f)P_f - \tau P_f W_p = 0, \\ \rho P_f - \mu_f G_f = 0, \\ \kappa \tau P_f W_p - \mu_f W_p = 0, \end{cases} \quad (24)$$

we obtain that the disease-free equilibrium of model (7) is given by

$$E_1^0 = \left(\frac{\Pi}{\mu_h}, 0, 0, 0, \frac{\mu_f}{\kappa \tau}, \frac{\rho}{\kappa \tau}, \frac{\sigma \rho - (\rho + \mu_f)\mu_f}{\tau \mu_f} \right), \quad (25)$$

or

$$E_2^0 = \left(\frac{\Pi}{\mu_h}, 0, 0, 0, 0, 0, 0 \right), \quad (26)$$

while the endemic disease equilibrium point is $(S^*, A^*, I^*, D^*, P_f^*, G_f^*, W_p^*)$, where

$$S^* = \frac{\Pi k_1}{\lambda(k_1 - \xi)((1 - u) + k_1 \mu_h)}, \quad A^* = \frac{\lambda((1 - u)S)}{k_1}, \quad I^* = \frac{\eta A}{k_2}, \quad D^* = \frac{\psi(k_2 + \eta)A}{k_2 k_3}, \quad (27)$$

$$P_f^* = \frac{\mu_f}{\kappa \tau}, \quad G_f^* = \frac{\rho}{\kappa \tau}, \quad W_p^* = \frac{\rho(\sigma - \mu_f) - \mu_f^2}{\tau \mu_f}. \quad (28)$$

Let $\mathcal{H} = (S, E, I, D, P_f, G_f, W_p)^T$. Then one observes that

$$\frac{d\mathcal{H}}{dt} = \mathcal{F} - \mathcal{V}, \quad (29)$$

where

$$\mathcal{F} = \begin{bmatrix} 0 & 0 & 0 & 0 & 0 & 0 & 0 \\ \frac{(1-u)\vartheta\rho}{\kappa\tau} & 0 & 0 & 0 & 0 & \frac{(1-u)\vartheta\Pi}{\mu_h} & 0 \\ 0 & 0 & 0 & 0 & 0 & 0 & 0 \\ 0 & 0 & 0 & 0 & 0 & 0 & 0 \\ 0 & 0 & 0 & 0 & 0 & 0 & 0 \\ 0 & 0 & 0 & 0 & 0 & 0 & 0 \\ 0 & 0 & 0 & 0 & 0 & 0 & 0 \end{bmatrix}, \quad (30)$$

$$\mathcal{V} = \begin{bmatrix} \frac{(1-u)\vartheta\rho}{\kappa\tau} + \mu_h & -\xi & 0 & 0 & 0 & \frac{(1-u)\vartheta\Pi}{\mu_h} & 0 \\ 0 & k_1 & 0 & 0 & 0 & 0 & 0 \\ 0 & -\eta & k_2 & 0 & 0 & 0 & 0 \\ 0 & -\psi & -\psi & k_3 & 0 & 0 & 0 \\ 0 & 0 & 0 & k_4 & -\sigma & \frac{\mu_f}{\kappa} & 0 \\ 0 & 0 & 0 & -\rho & \mu_f & 0 & 0 \\ 0 & 0 & 0 & 0 & -\kappa\tau \frac{\sigma\rho - (\rho + \mu_f)\mu_f}{\tau\mu_f} & 0 & 0 \end{bmatrix}. \quad (31)$$

The food-borne diseases reproduction number is given by

$$\mathcal{R}_0 = \rho(\mathcal{F}\mathcal{V}^{-1}) \quad (32)$$

with $\rho(\cdot)$ representing the spectral radius, from which we obtain

$$\mathcal{R}_0 = \frac{\xi\rho\vartheta(1-u)}{k_1\rho\vartheta(1-u) + \kappa k_1\tau\mu_h}. \quad (33)$$

3.5. Existence and Uniqueness

We reformulate the right-hand side of model (10) as follows:

$$\left\{ \begin{array}{l} \mathcal{M}_1(t, S, A, I, D, P_f, G_f, W_p) = \Pi + \xi A - (1-u)\lambda S - \mu_h S, \\ \mathcal{M}_2(t, S, A, I, D, P_f, G_f, W_p) = (1-u)\lambda S - (\mu_h + \eta + \xi)A, \\ \mathcal{M}_3(t, S, A, I, D, P_f, G_f, W_p) = \eta A - (\mu_h + \delta)I, \\ \mathcal{M}_4(t, S, A, I, D, P_f, G_f, W_p) = \psi(A + I) - ((1-u) + \theta + \gamma)D, \\ \mathcal{M}_5(t, S, A, I, D, P_f, G_f, W_p) = \sigma G_f - (\rho + \mu_f)P_f - \tau P_f W_p, \\ \mathcal{M}_6(t, S, A, I, D, P_f, G_f, W_p) = \rho P_f - \mu_f G_f, \\ \mathcal{M}_7(t, S, A, I, D, P_f, G_f, W_p) = \kappa\tau P_f W_p - \mu_f W_p. \end{array} \right. \quad (34)$$

From (34), our proposed model (10) can be expressed as

$$\left\{ \begin{array}{l} {}^C_0 D_t^\alpha \mathcal{M}(t) = \Phi(t, \mathcal{M}(t)), \quad t \in [0, \eta], \quad 0 < \alpha \leq 1, \\ \mathcal{M}(0) = \mathcal{M}_0, \end{array} \right. \quad (35)$$

where

$$\mathcal{M}(t) = \begin{pmatrix} S(t), \\ A(t), \\ I(t), \\ D(t), \\ P_f(t), \\ G_f(t), \\ W_p(t), \end{pmatrix} \quad \mathcal{M}_0 = \begin{pmatrix} S(0), \\ A(0), \\ I(0), \\ D(0), \\ P_f(0), \\ G_f(0), \\ W_p(0), \end{pmatrix} \quad (36)$$

and

$$\Phi(t, \mathcal{M}(t)) = \begin{cases} \mathcal{M}_1(t, S, A, I, D, P_f, G_f, W_p), \\ \mathcal{M}_2(t, S, A, I, D, P_f, G_f, W_p), \\ \mathcal{M}_3(t, S, A, I, D, P_f, G_f, W_p), \\ \mathcal{M}_4(t, S, A, I, D, P_f, G_f, W_p), \\ \mathcal{M}_5(t, S, A, I, D, P_f, G_f, W_p), \\ \mathcal{M}_6(t, S, A, I, D, P_f, G_f, W_p), \\ \mathcal{M}_7(t, S, A, I, D, P_f, G_f, W_p). \end{cases} \quad (37)$$

Using the ideas in Lemma 2.1, system (35) yields

$$\mathcal{M}(t) = \mathcal{M}_0(t) + \frac{1}{\Gamma(\alpha)} \int_0^t \Phi(s, \mathcal{M}(s))(t-s)^{\alpha-1} ds. \quad (38)$$

Further, we let $0 \leq t \leq \mathcal{T}$ with the Banach space $\mathcal{B} = C([0, \mathcal{T}] \times \mathbb{R}_+^7, \mathbb{R}_+)$ under the norm

$$\|\mathcal{M}\|_{\mathcal{B}} = \|(S, A, I, D, P_f, G_f, W_p)\|_{\mathcal{B}} = \sup\{|\mathcal{D}(t)| : t \in \mathcal{T}\}, \quad (39)$$

such that

$$|\mathcal{D}| := |S| + |A| + |I| + |D| + |P_f| + |G_f| + |W_p|. \quad (40)$$

For obtaining existence and uniqueness, we assume some growth conditions on function vector

$$m : [0, \mathcal{T}] \times \mathbb{R}_+^7 \longrightarrow \mathbb{R}_+ \quad (41)$$

as: $(F_1) \exists Q_m, C_m$ such that

$$\Phi(t, \mathcal{M}(t)) \leq Q_m |\mathcal{M}| + C_m. \quad (42)$$

$(F_2) \exists \mathbf{L}_m > 0$ such that if $\mathcal{M}, \tilde{\mathcal{M}} \in \mathcal{B}$, then

$$|\Phi(t, \mathcal{M}(t)) - \Phi(t, \tilde{\mathcal{M}}(t))| \leq \mathbf{L}_m \|\mathcal{M} - \tilde{\mathcal{M}}\|. \quad (43)$$

Theorem 3.1. *Under the continuity of m together with (F_1) , system (35) has at least one solution.*

Proof. We shall arrive at the required conclusion using the Schauder fixed point theorem. Let us take a closed subset \mathcal{Z} of \mathcal{B} as $\mathbf{T}_{\Omega} = \{\mathcal{M} \in \mathcal{B} : \|\mathcal{M}\| \leq \mathbb{R}, \mathbb{R} > 0\}$, where \mathbf{T}_{Ω} is the operator defined as $\mathbf{T}_{\Omega} : \mathcal{Z} \rightarrow \mathcal{Z}$ such that

$$\mathbf{T}_{\Omega}(\mathcal{M}) = \mathcal{M}_0(t) + \frac{1}{\Gamma(\alpha)} \int_0^t \Phi(s, \mathcal{M}(s))(t-s)^{\alpha-1} ds, \quad (44)$$

which means that

$$\begin{aligned} |\mathbf{T}_{\Omega}(\mathcal{M})(t)| &\leq |\mathcal{M}_0| + \frac{1}{\Gamma(\alpha)} \int_0^t |\Phi(s, \mathcal{M}(s))|(t-s)^{\alpha-1} ds, \\ &\leq |\mathcal{M}_0| + \frac{1}{\Gamma(\alpha)} \int_0^t (t-s)^{\alpha-1} [Q_m |\mathcal{M}| + C_m] ds, \\ &\leq |\mathcal{M}_0| + \frac{\mathcal{T}^{\alpha}}{\Gamma(\alpha+1)} [Q_m \|\mathcal{M}\| + C_m]. \end{aligned} \quad (45)$$

From (45), it follows that $|\mathbf{T}_\Omega(\mathcal{M})| \leq |\mathcal{M}_0| + \frac{\mathcal{T}^\alpha}{\Gamma(\alpha+1)}[Q_m\|\mathcal{M}\| + C_m]$ and also $\mathbf{T}_\Omega \in \mathcal{Z}$ such that $\mathbf{T}_\Omega(\mathcal{Z}) \subset \mathcal{Z}$. Also it reveals that the operator \mathbf{T}_Ω is bounded. For completely continuity we proceed as follows. Let $t_2 < t_1 \in [0, \mathcal{T}]$ such that

$$\begin{aligned} |\mathbf{T}_\Omega(\mathcal{M})(t_2)| - |\mathbf{T}_\Omega(\mathcal{M})(t_1)| &\leq \left| \frac{1}{\Gamma(\alpha)} \int_0^{t_2} \Phi(s, \mathcal{M}(s))(t_2 - s)^{\alpha-1} ds \right. \\ &\quad \left. - \frac{1}{\Gamma(\alpha)} \int_0^{t_1} \Phi(s, \mathcal{M}(s))(t_1 - s)^{\alpha-1} ds \right| \\ &\leq \frac{1}{\Gamma(\alpha)} \left[\int_0^{t_1} [(t_1 - s)^{\alpha-1} - (t_2 - s)^{\alpha-1}] \Phi(s, \mathcal{M}(s)) ds \right. \\ &\quad \left. + \int_{t_1}^{t_2} (t_2 - s)^{\alpha-1} \Phi(s, \mathcal{M}(s)) ds \right], \\ &\leq \frac{Q_m \mathcal{R} + C_m}{\Gamma(\alpha+1)} [(t_2^\alpha - t_1^\alpha) + 2(t_2 - t_1)^\alpha]. \end{aligned} \quad (46)$$

Basically, we can see from (46) that $|\mathbf{T}_\Omega(\mathcal{M})(t_2)| - |\mathbf{T}_\Omega(\mathcal{M})(t_1)| \rightarrow 0$ as $t_2 \rightarrow t_1$. Hence, \mathbf{T}_Ω is an equicontinuous operator. With the help of the Arzela Ascoli theorem, we know that function \mathbf{T}_Ω is a completely continuous function and uniformly bounded. Again, by Schauder's fixed point theorem, we conclude that our proposed system has at least one solution. \square

Theorem 3.2. *Suppose that (F_2) holds. Then the considered system (35) has a unique solution if*

$$\frac{\mathcal{T}^\alpha}{\Gamma(\alpha+1)} \mathbf{L}_m < 1. \quad (47)$$

Proof. If $\mathcal{M}, \tilde{\mathcal{M}} \in \mathcal{B}$, then

$$\begin{aligned} \|\mathbf{T}_\Omega(\mathcal{M}) - \mathbf{T}_\Omega(\tilde{\mathcal{M}})\| &\leq \sup_{t \in [0, \mathcal{T}]} \left| \frac{1}{\Gamma(\alpha)} \int_0^t \Phi(s, \mathcal{M}(s))(t - s)^{\alpha-1} ds \right. \\ &\quad \left. - \frac{1}{\Gamma(\alpha)} \int_0^t \Phi(s, \tilde{\mathcal{M}}(s))(t - s)^{\alpha-1} ds \right|, \\ &\leq \frac{\mathcal{T}^\alpha}{\Gamma(\alpha+1)} \mathbf{L}_m \|\mathcal{M} - \tilde{\mathcal{M}}\|. \end{aligned} \quad (48)$$

Hence, $\|\mathbf{T}_\Omega(\mathcal{M}) - \mathbf{T}_\Omega(\tilde{\mathcal{M}})\| \leq \frac{\mathcal{T}^\alpha}{\Gamma(\alpha+1)} \mathbf{L}_m \|\mathcal{M} - \tilde{\mathcal{M}}\|$, which completes the proof: from the contraction principle, the operator has a unique fixed point and, consequently, our proposed model has a unique solution. \square

3.6. Hyers-Ulam Stability (HU)

The stability of numerical results of our proposed system will be examined in this section.

Lemma 3.2. *The solution $\mathcal{M}(t)$ of*

$$\begin{aligned} {}^C_0 D_t^\alpha \mathcal{M}(t) &= \Phi(t, \mathcal{M}(t)) + \Upsilon(t), \\ \mathcal{M}(0) &= \mathcal{M}_0, \end{aligned} \quad (49)$$

satisfies the relation

$$\left| \mathcal{M}(t) - \left(\mathcal{M}_0(t) + \frac{1}{\Gamma(\alpha)} \int_0^t \Phi(s, \mathcal{M}(s))(t - s)^{\alpha-1} ds \right) \right| \leq \frac{\mathcal{T}^\alpha}{\Gamma(\alpha+1)} \epsilon = \Delta \epsilon. \quad (50)$$

Proof. The proof is standard and we omit it here. \square

Theorem 3.3. *Suppose that assumption (F_2) together with (46) hold. Then the solution of the integral (37) is Hyers-Ulam (HU) stable and, consequently, the numerical results of the considered model are HU stable if*

$$\Theta = \frac{\mathcal{T}^\alpha}{\Gamma(\alpha + 1)} \mathbf{L}_m < 1. \quad (51)$$

Proof. Let $\mathcal{M} \in \mathcal{B}$ be any solution and $\tilde{\mathcal{M}} \in \mathcal{B}$ be the unique solution of (37). Then,

$$\begin{aligned} |\mathcal{M}(t) - \tilde{\mathcal{M}}(t)| &= \left| \mathcal{M}(t) - \left(\mathcal{M}_0(t) + \frac{1}{\Gamma(\alpha)} \int_0^t \Phi(s, \tilde{\mathcal{M}}(s))(t-s)^{\alpha-1} ds \right) \right| \\ &\leq \left| \mathcal{M}(t) - \left(\mathcal{M}_0(t) + \frac{1}{\Gamma(\alpha)} \int_0^t \Phi(s, \tilde{\mathcal{M}}(s))(t-s)^{\alpha-1} ds \right) \right| \\ &\quad + \left| \frac{1}{\Gamma(\alpha)} \int_0^t \Phi(s, \tilde{\mathcal{M}}(s))(t-s)^{\alpha-1} ds - \frac{1}{\Gamma(\alpha)} \int_0^t \Phi(s, \tilde{\mathcal{M}}(s))(t-s)^{\alpha-1} ds \right| \\ &\leq \Delta\epsilon + \Theta |\mathcal{M} - \tilde{\mathcal{M}}|. \end{aligned} \quad (52)$$

Thus,

$$|\mathcal{M} - \tilde{\mathcal{M}}| \leq \frac{\Delta}{1 - \Theta} \epsilon.$$

Hence, we conclude that system (37) is HU stable. \square

4. Numerical Scheme

The fractional predictor-corrector approach, which was established and examined for its convergence and error bounds in [23], is a numerical explicit technique used to test the performance of the suggested fractional-order model (7) under the Caputo differential operator. Let us consider

$$\begin{cases} {}^C D_t^\alpha \mathcal{M}(t) = \Phi(t, \mathcal{M}(t)), \\ \mathcal{M}(0) = \mathcal{M}_0. \end{cases} \quad (53)$$

Choose the step length $h = \frac{T}{M}$, where M is a positive integer and T is the upper limit of the closed interval of integration $[0, T]$. Using the integral equation equivalent to system (10), $\mathcal{M}_a(t_{j+1})$, $j = 0, 1, \dots, n$, can be calculated by

$$\mathcal{M}_a(t_{j+1}) = \frac{h^\alpha}{\Gamma(\alpha + 2)} \left[\sum_{j=0}^n d_{j,n+1} \Phi(t_j, \mathcal{M}_a(t_j)) + \Phi(t_{n+1}, \mathcal{M}_a^p(t_{n+1})) \right] + \mathcal{M}_0,$$

where

$$d_{j,n+1} = \begin{cases} n^{\alpha+1} - (n - \alpha)(n + 1)^\alpha, & j = 0, \\ (n - j + 2)^{\alpha+1} + (n - j)^{\alpha+1} - 2(n - j + 1)^{\alpha+1}, & 1 \leq j \leq n, \\ 1, & j = n + 1. \end{cases}$$

The predictor formula is derived as follows:

$$\mathcal{M}_a^p(t_{n+1}) = \frac{1}{\Gamma(\alpha+1)} \sum_{j=0}^n h^\alpha [(n-j+1)^\alpha - (n-j)^\alpha] \Phi(t_j, \mathcal{M}_a(t_j)) + \mathcal{M}_0.$$

Thus the corrector formula for system (10) is

$$\begin{aligned} {}^C_0 D_t^\alpha S(t_{j+1}) &= \frac{\mathbf{h}^\alpha}{\Gamma(\alpha+2)} \left[\sum_{j=0}^n d_{j,n+1} \Phi_1(t_j, \mathcal{M}_a(t_j)) + \Phi_1(t_{n+1}, \mathcal{M}_a^p(t_{n+1})) \right] + S_0, \\ {}^C_0 D_t^\alpha A(t_{j+1}) &= \frac{\mathbf{h}^\alpha}{\Gamma(\alpha+2)} \left[\sum_{j=0}^n d_{j,n+1} \Phi_2(t_j, \mathcal{M}_a(t_j)) + \Phi_2(t_{n+1}, \mathcal{M}_a^p(t_{n+1})) \right] + A_0, \\ {}^C_0 D_t^\alpha I(t_{j+1}) &= \frac{\mathbf{h}^\alpha}{\Gamma(\alpha+2)} \left[\sum_{j=0}^n d_{j,n+1} \Phi_3(t_j, \mathcal{M}_a(t_j)) + \Phi_3(t_{n+1}, \mathcal{M}_a^p(t_{n+1})) \right] + I_0, \\ {}^C_0 D_t^\alpha D(t_{j+1}) &= \frac{\mathbf{h}^\alpha}{\Gamma(\alpha+2)} \left[\sum_{j=0}^n d_{j,n+1} \Phi_4(t_j, \mathcal{M}_a(t_j)) + \Phi_4(t_{n+1}, \mathcal{M}_a^p(t_{n+1})) \right] + D_0, \\ {}^C_0 D_t^\alpha P_f(t_{j+1}) &= \frac{\mathbf{h}^\alpha}{\Gamma(\alpha+2)} \left[\sum_{j=0}^n d_{j,n+1} \Phi_5(t_j, \mathcal{M}_a(t_j)) + \Phi_5(t_{n+1}, \mathcal{M}_a^p(t_{n+1})) \right] + P_{f_0}, \\ {}^C_0 D_t^\alpha G_f(t_{j+1}) &= \frac{\mathbf{h}^\alpha}{\Gamma(\alpha+2)} \left[\sum_{j=0}^n d_{j,n+1} \Phi_6(t_j, \mathcal{M}_a(t_j)) + \Phi_6(t_{n+1}, \mathcal{M}_a^p(t_{n+1})) \right] + G_{f_0}, \\ {}^C_0 D_t^\alpha W_p(t_{j+1}) &= \frac{\mathbf{h}^\alpha}{\Gamma(\alpha+2)} \left[\sum_{j=0}^n d_{j,n+1} \Phi_7(t_j, \mathcal{M}_a(t_j)) + \Phi_7(t_{n+1}, \mathcal{M}_a^p(t_{n+1})) \right] + W_{p_0}. \end{aligned}$$

The results of this iterative scheme are given in Section 5.

5. Results

For the purpose of validating our created iterative scheme, we now present some numerical simulations. For this, we start by assuming initial values for each compartment of our proposed model (7), thus: $S = 500000$; $A = 300000$; $I = 3500$; $D = 2000$; $P_f = 250000$; $G_f = 200000$; $W_p = 2000$. Figure 3 shows the Latin hypercube sampling of the parameters in the control reproduction number. It is noticed that the following parameters (temporal resistance rate, the rate at which pupae of flies move to adult flies, and infectivity rate of adult flies) contribute positively to the spread of food-borne diseases and increase in these parameters (local government interventions, the rate at which the asymptomatic become infected, proportionality constant, reduction coefficient of pupae of flies and parasitic wasps due to the interaction, and natural death rate for human) reduces the spread of food-borne diseases. We have employed the Predictor-Corrector scheme of Section 4 to obtain a numerical solution to the system. We compare the effects of various fractional order values with of a step size 0.2 throughout the time range $[0,300]$ against

the suitable parameter values listed in Table 1. We deduced from all of the graphical simulations that the Caputo fractional derivative efficiently describes the intricate dynamics of the presented model of food-borne diseases.

5.1. Sensitivity analysis

Now, we utilize sensitivity analysis to determine the relative significance of each model parameter in the reproduction number of food-borne diseases, denoted as \mathcal{R}_0 , by referring to the data provided in Table 1. The current objective is to ascertain the influence of alterations in the model parameters on the reproduction number of food-borne diseases. Similar instances may be found in the work of [12, 11, 13]. We generate a three-dimensional graph representing the natural mortality rate for humans and flies, the constant of proportionality, the rate of temporal resistance, the reduction coefficient of $P_f(t)$ and $W_p(t)$ resulting from their interaction, the rate at which $P_f(t)$ transitions to $G_f(t)$, and the intervention by local government, presented in Fig. 2. In addition, the Latin Hypercube Sampling (LHS) technique was utilized to generate 2000 samples from a uniform distribution. These samples were used to determine the global sensitivity of the different generic factors in the food illnesses reproduction number. The resulting sensitivity analysis is depicted in Fig. 3.

6. Discussion

The fractional differential model provides the best fits to study such epidemic scenarios because they give us more options to replicate the structure, both theoretically and practically. Fig. 4 and Fig. 5 represent the numerical simulation results for the human and flies populations. It is clear that the outcomes and the changes of the fractional-order α fit well, which indicate that the method is effective, thus when the operator varies by changing α , the dynamism of each state variable have the same trend. From Fig. 4(a)–4(d), we see that when the fractional order α is reduced to 1, all the human compartments increase significantly. The biological or real-life meaning of this dynamics is that urbanization, busy schedules, and a lack of time to prepare meals, as well as the convenience of the process, time-saving benefits, and accessibility to information on all food types, menus, and prices, all contribute to the rising popularity of online food ordering and delivery in numerous nations. The profit or benefit of food delivery comes however with a high risk of food safety challenge to the already existing food safety challenges of the ready-to-eat food, which leads to high susceptibility and infectivity of food-borne diseases. In Fig. 5(a)–5(c), we see that the dynamics of flies development goes through four stages in the aquatic environment, including egg, larvae, pupae, and adult fly population. Any control intervention, at any stage, results in the management of adult flies in the area under consideration. The flies mature in this filthy habitat and become free to wander around the neighbouring housing communities, where they spread the bacteria

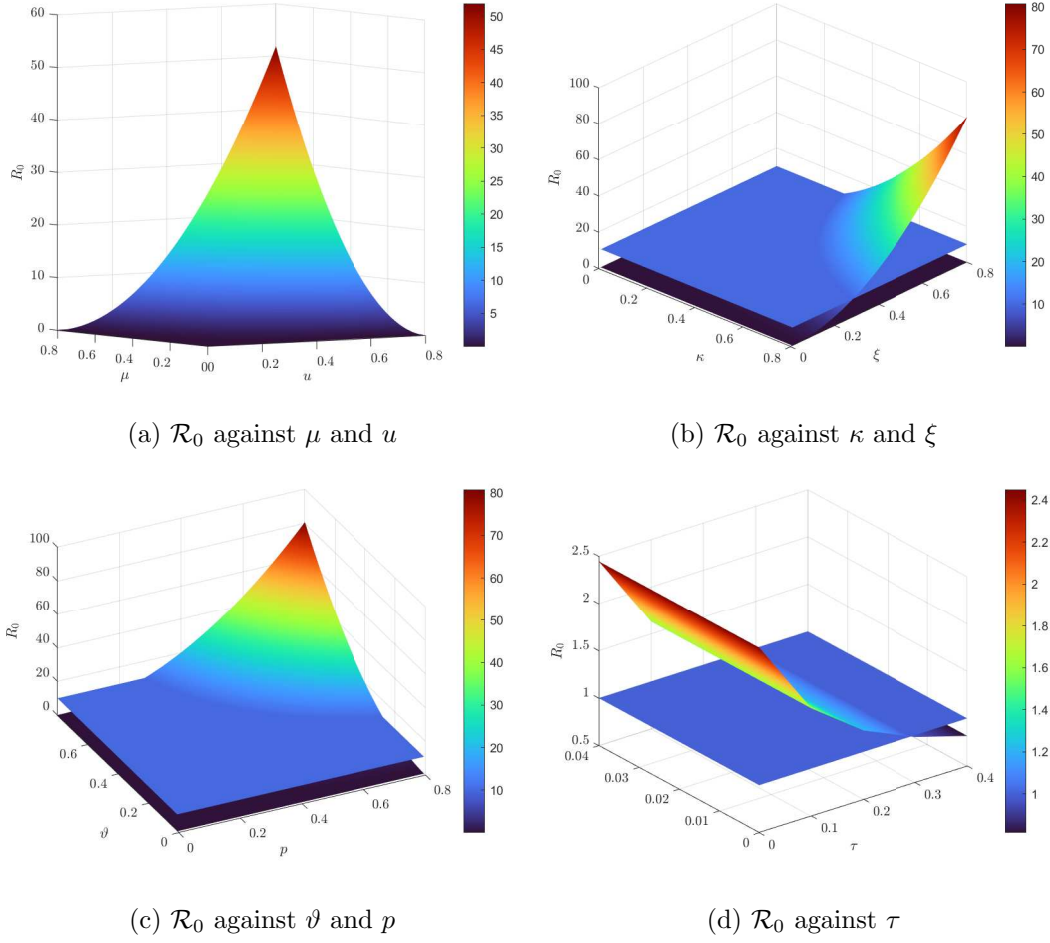


Fig. 2: Dynamics of \mathcal{R}_0 on various parameters.

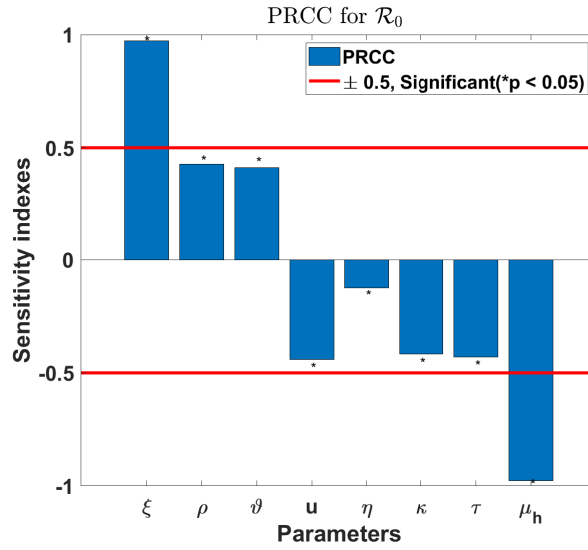


Fig. 3: Sensitivity plot

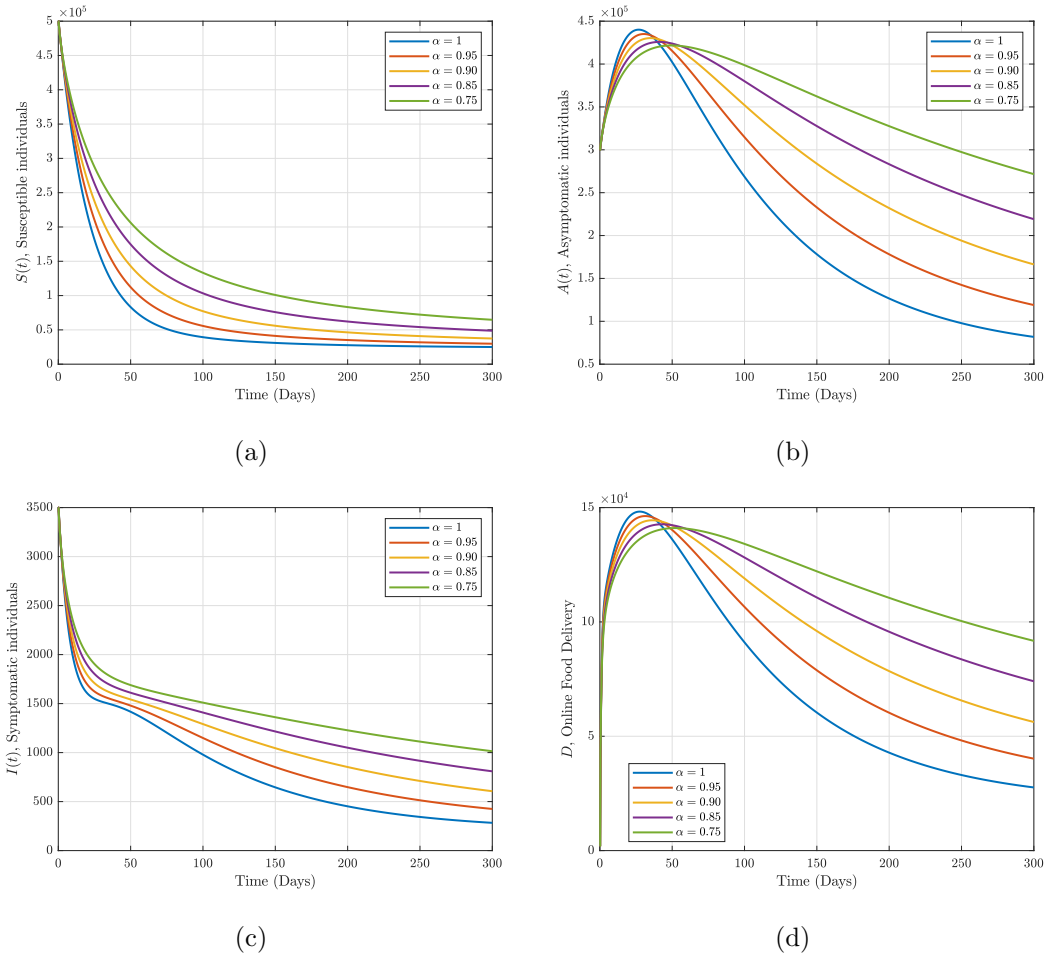


Fig. 4: Numerical trajectory of food-borne diseases transmission under Caputo fractional operator.

that cause various food-borne diseases. In Fig. 6(a)–6(d), we show the numerical sensitivity of food-borne diseases transmission for humans under the Caputo fractional operator with order $\alpha = 0.95$, when the rate of government intervention coverage is varied. We observe that as the rate of government intervention coverage increases, there is a decline in the number of asymptomatic and symptomatic infected humans, and a little increase in the number of susceptible humans and online food delivery. This result gives chance to the government to implement any food safety control intervention to the maximum since it will not affect the order-delivery food but reduce infection. In Fig. 7, we show the numerical sensitivity of ψ and θ on online food delivery under the Caputo fractional operator with order $\alpha = 0.95$. We note that as the rate of ψ and θ increase, there is a high decrease in the online food delivery compartment of the model. From a biological point of view, these observations suggest that the memories of environmental hygiene and disease inflow may reduce food-borne diseases transmission.

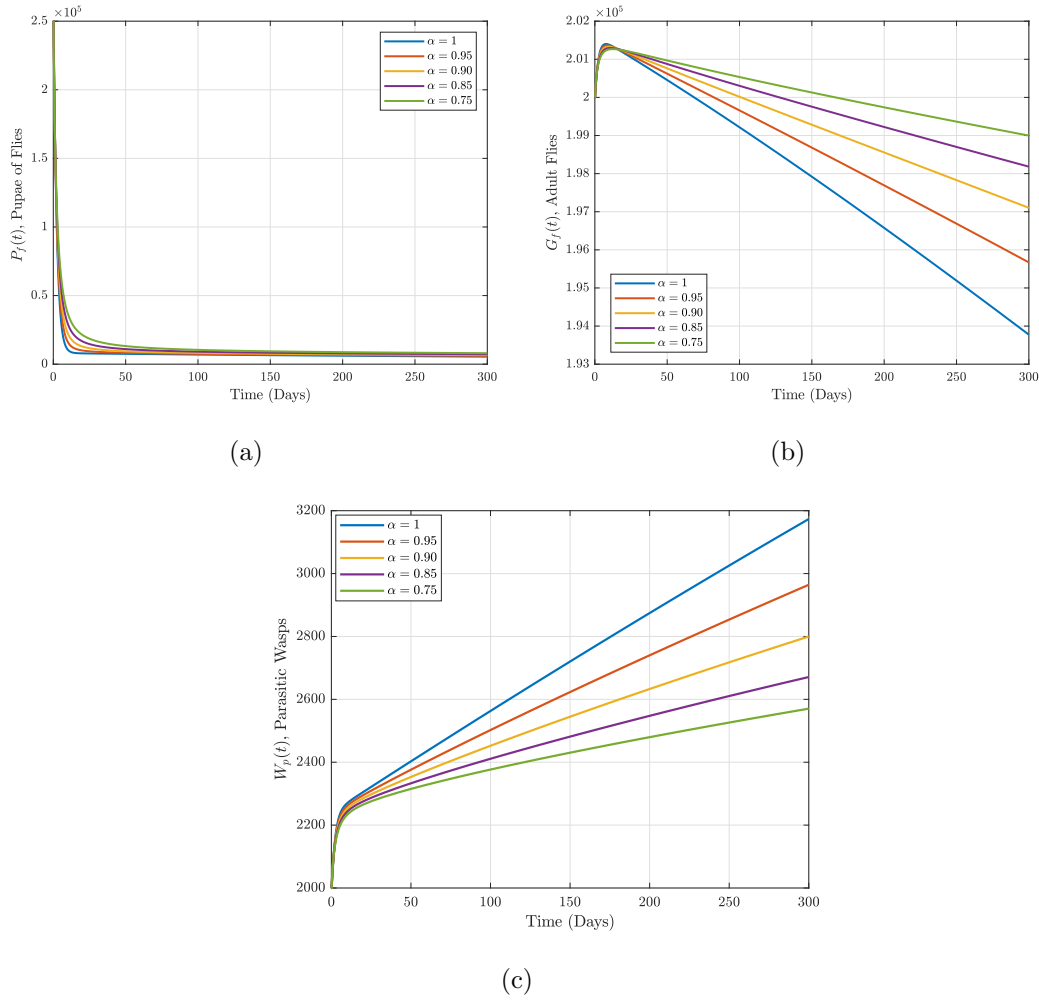


Fig. 5: Numerical trajectory of food-borne diseases transmission under the Caputo fractional operator.

7. Conclusion

We have proposed and comprehensively analyzed a novel deterministic mathematical model for the transmission of food-borne diseases in a population consisting of humans and flies, considering the Caputo fractional order derivative and employing a Predictor-Corrector scheme. The qualitative aspects of the model, including positivity, boundedness, equilibrium points, and the basic reproductive number, have been thoroughly investigated. The analysis of system existence and uniqueness has been carried out using the Banach and Schauder fixed point theorems. Additionally, the stability of the fractional controlling system of equations has been examined using Hyers-Ulam-type stability criteria. To assess the efficacy of the proposed fractional-order model, numerical trajectories have been generated. We have also examined the impact of critical parameters. Based on these trajectories, we have hypothesized that the memory index or fractional order could be utilized by public health policymakers to comprehend and predict the dynamics of food-borne disease transmission. Furthermore, we have observed that maximum implemen-

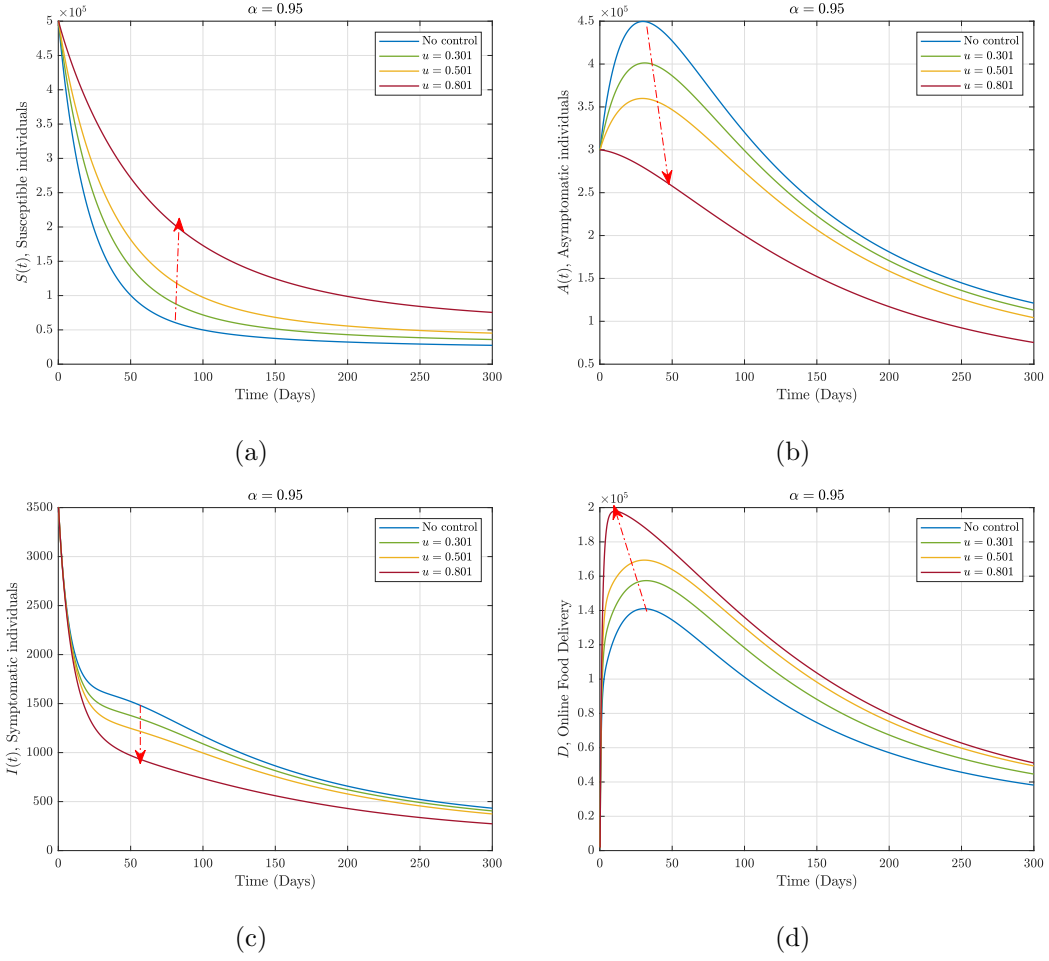


Fig. 6: Numerical comparison of government control when $\alpha = 0.95$.

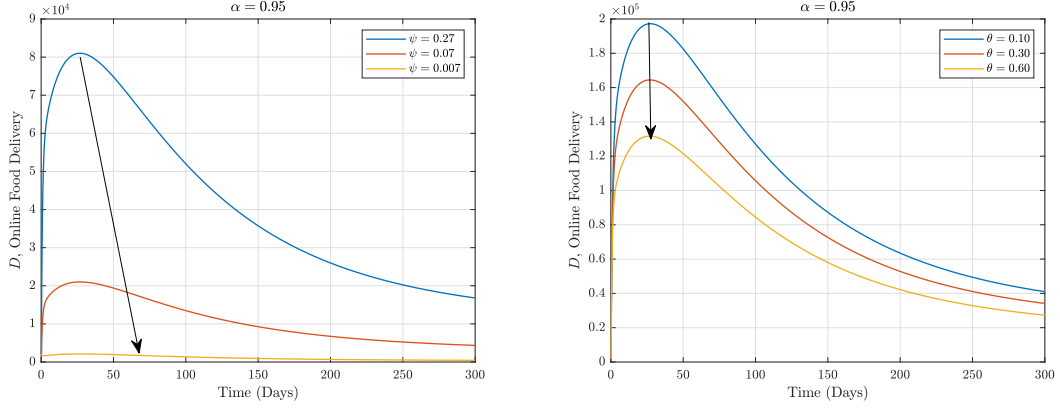


Fig. 7: Numerical comparison of ψ and θ when $\alpha = 0.95$.

tation of food safety control interventions by the government may not have an effect on food delivery services. Additionally, we have found that improvements in environmental hygiene and the reduction of disease inflow can potentially decrease the incidence of food-borne diseases.

Acknowledgements

This work was partially supported by the Fundação para a Ciência e a Tecnologia, I.P. (FCT, Funder ID = 50110000187) under grants UIDB/04106/2020 and UIDP/04106/2020 (CIDMA); and project 2022.03091.PTDC (CoSysM3).

Author contributions

The authors confirm sole responsibility for study conceptualization, methodology, formal analysis, codes writing, manuscript writing and editing, and approval of the final manuscript.

Declarations

Funding

This work was partially supported by the Fundação para a Ciência e a Tecnologia, I.P. (FCT, Funder ID = 50110000187) under grants UIDB/04106/2020 and UIDP/04106/2020 (CIDMA); and project 2022.03091.PTDC (CoSysM3).

Competing interests

The authors have no competing interests to declare that are relevant to the content of this article.

Availability of data and materials

The authors confirm that the data supporting the findings of this study are available within the article.

Code availability

Matlab code is available from the corresponding author on reasonable request.

References

- [1] Abidemi, A. (2023). Optimal cost-effective control of drug abuse by students: insight from mathematical modeling. *Modeling Earth Systems and Environment*, 9, 811–829.
- [2] Addai, E., Zhang, L., Asamoah, J. K., and Essel, J. F. (2023). A fractional order age-specific smoke epidemic model. *Applied Mathematical Modelling*, 119, 99–118.
- [3] Ahmad, Y. U., Andrawus, J., Ado, A., Maigoro, Y. A., Yusuf, A., Althobaiti, S., and Mustapha, U. T. (2024). Mathematical modeling and analysis of human-to-human monkeypox virus transmission with post-exposure vaccination. *Modeling Earth Systems and Environment*, (pp. 1–21).

- [4] Ahmed, I., Baba, I. A., Yusuf, A., Kumam, P., and Kumam, W. (2020). Analysis of caputo fractional-order model for covid-19 with lockdown. *Advances in difference equations*, 2020, 394.
- [5] Ain, Q. T., Anjum, N., Din, A., Zeb, A., Djilali, S., and Khan, Z. A. (2022). On the analysis of caputo fractional order dynamics of middle east lungs coronavirus (mers-cov) model. *Alexandria Engineering Journal*, 61, 5123–5131.
- [6] Alade, T. O., Alnegga, M., Olaniyi, S., and Abidemi, A. (2023). Mathematical modelling of within-host chikungunya virus dynamics with adaptive immune response. *Modeling Earth Systems and Environment*, 9, 3837–3849.
- [7] Aldila, D., Götz, T., and Soewono, E. (2013). An optimal control problem arising from a dengue disease transmission model. *Mathematical biosciences*, 242, 9–16.
- [8] Alla Hamou, A., Azroul, E., Bouda, S., and Guedda, M. (2024). Mathematical modeling of hiv transmission in a heterosexual population: incorporating memory conservation. *Modeling Earth Systems and Environment*, 10, 393–416.
- [9] Anastassopoulou, C., Russo, L., Tsakris, A., and Siettos, C. (2020). Data-based analysis, modelling and forecasting of the covid-19 outbreak. *PloS one*, 15, e0230405.
- [10] Anderson, R. M., and May, R. M. (1991). *Infectious diseases of humans: dynamics and control*. Oxford university press.
- [11] Asamoah, J. K. K., Jin, Z., and Sun, G.-Q. (2021). Non-seasonal and seasonal relapse model for q fever disease with comprehensive cost-effectiveness analysis. *Results in Physics*, 22, 103889.
- [12] Asamoah, J. K. K., Jin, Z., Sun, G.-Q., Seidu, B., Yankson, E., Abidemi, A., Oduro, F., Moore, S. E., and Okyere, E. (2021). Sensitivity assessment and optimal economic evaluation of a new covid-19 compartmental epidemic model with control interventions. *Chaos, Solitons and Fractals*, 146, 110885.
- [13] Asamoah, J. K. K., and Sun, G.-Q. (2023). Fractional caputo and sensitivity heat map for a gonorrhea transmission model in a sex structured population. *Chaos, Solitons and Fractals*, 175, 114026.
- [14] Aslam, M., Murtaza, R., Abdeljawad, T., Rahman, G. u., Khan, A., Khan, H., and Gulzar, H. (2021). A fractional order hiv/aids epidemic model with mittag-leffler kernel. *Advances in Difference Equations*, 2021, 1–15.

- [15] Ball, F. G., Knock, E. S., and O'Neill, P. D. (2008). Control of emerging infectious diseases using responsive imperfect vaccination and isolation. *Math. Biosci.*, *216*, 100–113. URL: <https://doi.org/10.1016/j.mbs.2008.08.008>. doi:10.1016/j.mbs.2008.08.008.
- [16] Barro, M., Guiro, A., and Ouedraogo, D. (2018). Optimal control of a sir epidemic model with general incidence function and a time delays. *Cubo (Temuco)*, *20*, 53–66.
- [17] Becker, N. (1979). The uses of epidemic models. *Biometrics*, (pp. 295–305).
- [18] Brauer, F., and Castillo-Chavez, C. (2012). *Mathematical models in population biology and epidemiology* volume 40 of *Texts in Applied Mathematics*. (2nd ed.). Springer, New York. URL: <https://doi.org/10.1007/978-1-4614-1686-9>. doi:10.1007/978-1-4614-1686-9.
- [19] Caputo, M., and Fabrizio, M. (2015). A new definition of fractional derivative without singular kernel. *Progress in Fractional Differentiation and Applications*, *1*, 73–85.
- [20] Casella, F. (2020). Can the covid-19 epidemic be controlled on the basis of daily test reports? *IEEE Control Systems Letters*, *5*, 1079–1084.
- [21] Castilho, C. (2006). Optimal control of an epidemic through educational campaigns. *Electronic Journal of Differential Equations (EJDE)[electronic only]*, *2006*, Paper–No.
- [22] Diethelm, K. (2013). A fractional calculus based model for the simulation of an outbreak of dengue fever. *Nonlinear Dynamics*, *71*, 613–619.
- [23] Diethelm, K., Ford, N. J., and Freed, A. D. (2004). Detailed error analysis for a fractional adams method. *Numerical algorithms*, *36*, 31–52.
- [24] Djordjevic, J., Silva, C. J., and Torres, D. F. M. (2018). A stochastic SICA epidemic model for HIV transmission. *Applied Mathematics Letters*, *84*, 168–175.
- [25] Giles-Corti, B., Vernez-Moudon, A., and Reis, R. (2016). City planning and population health: a global challenge. *Lancet.*, *388*, 2912–2924. URL: [http://dx.doi.org/10.1016/S0140-6736\(16\)30066-6](http://dx.doi.org/10.1016/S0140-6736(16)30066-6).
- [26] González-Parra, G., Arenas, A. J., and Chen-Charpentier, B. M. (2014). A fractional order epidemic model for the simulation of outbreaks of influenza a (h1n1). *Mathematical methods in the Applied Sciences*, *37*, 2218–2226.
- [27] Khan, M. A., Hammouch, Z., and Baleanu, D. (2019). Modeling the dynamics of hepatitis e via the caputo–fabrizio derivative. *Mathematical Modelling of Natural Phenomena*, *14*, 311.

- [28] Kumar, S., Chauhan, R., Momani, S., and Hadid, S. (2024). Numerical investigations on covid-19 model through singular and non-singular fractional operators. *Numerical Methods for Partial Differential Equations*, 40, e22707.
- [29] Mugabi, F., Duffy, K. J., and van Langevelde, F. (2024). Behaviours of honeybees can reduce the probability of deformed wing virus outbreaks in varroa destructor-infested colonies. *Modeling Earth Systems and Environment*, (pp. 1–17).
- [30] Mustapha, U. T., Qureshi, S., Yusuf, A., and Hincal, E. (2020). Fractional modeling for the spread of hookworm infection under caputo operator. *Chaos, Solitons and Fractals*, 137, 109878.
- [31] Ndaïrou, F., Area, I., Nieto, J. J., Silva, C. J., and Torres, D. F. M. (2018). Mathematical modeling of Zika disease in pregnant women and newborns with microcephaly in Brazil. *Mathematical Methods in the Applied Sciences*, 41, 8929–8941.
- [32] Ndaïrou, F., Area, I., Nieto, J. J., and Torres, D. F. M. (2020). Mathematical modeling of Covid-19 transmission dynamics with a case study of Wuhan. *Chaos, Solitons and Fractals*, 135, 109846.
- [33] Noor, N. B., Yousefi, N., Spann, B., and Agarwal, N. (2023). Comparing toxicity across social media platforms for covid-19 discourse. In *IARIA Conference* (pp. 21–26). doi:10.48550/arXiv.2302.14270.
- [34] Peter, O. J., Kumar, S., Kumari, N., Oguntolu, F. A., Oshinubi, K., and Musa, R. (2022). Transmission dynamics of monkeypox virus: a mathematical modelling approach. *Modeling Earth Systems and Environment*, (pp. 1–12).
- [35] Peter, O. J., Oguntolu, F. A., Ojo, M. M., Olayinka Oyeniyi, A., Jan, R., and Khan, I. (2022). Fractional order mathematical model of monkeypox transmission dynamics. *Physica Scripta*, 97, 084005.
- [36] Podlubny, I. (1998). *Fractional differential equations: an introduction to fractional derivatives, fractional differential equations, to methods of their solution and some of their applications*. elsevier.
- [37] Rachah, A., and Torres, D. F. M. (2016). Dynamics and optimal control of Ebola transmission. *Mathematics in Computer Science*, 10, 331–342.
- [38] Sahu, I., and Jena, S. R. (2023). Sdiqr mathematical modelling for covid-19 of odisha associated with influx of migrants based on laplace adomian decomposition technique. *Modeling Earth Systems and Environment*, 9, 4031–4040.

- [39] Shaik, M., Yousefi, N., Agarwal, N., and Spann, B. (2023). Evaluating role of instagram’s multimedia in connective action leveraging diffusion of innovation and cognitive mobilization theories: Brazilian and Peruvian social unrest case studies. In *2023 10th International Conference on Behavioural and Social Computing (BESC)* (pp. 1–6). Larnaca, Cyprus. doi:10.1109/BESC59560.2023.10386436.
- [40] Sharma, A. K., Kumar, V., and Singh, R. N. (2023). A fractional treatment to food-borne disease modeling by q- homotopy analysis transform method (q-hatm). *IJARSCT*, 3.
- [41] Sher, M., Shah, K., Khan, Z. A., Khan, H., and Khan, A. (2020). Computational and theoretical modeling of the transmission dynamics of novel covid-19 under mittag-leffler power law. *Alexandria Engineering Journal*, 59, 3133–3147.
- [42] Statista (2021). Online food delivery. <https://www.statista.com/outlook/dmo/eservices/online-food-delivery/australia>.
- [43] Strategy, A. (2021). Making delivery work for everyone. <https://www.readkong.com/page/making-delivery-work-for-everyone-march-2021-accenture-8593927>.
- [44] Thabet, S. T., Abdo, M. S., Shah, K., and Abdeljawad, T. (2020). Study of transmission dynamics of covid-19 mathematical model under abc fractional order derivative. *Results in Physics*, 19, 103507.
- [45] Tilahun, G. T., Woldegerima, W. A., and Mohammed, N. (2021). A fractional order model for the transmission dynamics of hepatitis b virus with two-age structure in the presence of vaccination. *Arab Journal of Basic and Applied Sciences*, 28, 87–106.
- [46] UNTW (2022). The 2030 agenda for sustainable development: United nations. <https://sdgs.un.org/2030agenda>.
- [47] Yousefi, N. (2021). Exploring machine learning methods for predicting disease progression in colon cancer patients. URL: <https://etd.adm.unipi.it/t/etd-06102021-163040/>.
- [48] Yousefi, N., Noor, N. B., Spann, B., and Agarwal, N. (2023). Towards developing a measure to assess contagiousness of toxic tweets. In *TrueHealth 2023, Workshop on Combating Health Misinformation for Social Wellbeing*. In press.
- [49] Zhang, L., Addai, E., Ackora-Prah, J., Arthur, Y. D., Asamoah, J. K. K. et al. (2022). Fractional-order ebola-malaria coinfection model with a focus on detection and treatment rate. *Computational and Mathematical Methods in Medicine*, 2022.